Eur. Phys. J. B **44**, 57–62 (2005)
DOI: 10.1140/epjb/e2005-00099-1

THE EUROPEAN PHYSICAL JOURNAL B

# The influence of the second harmonic in the current-phase relation on the voltage-current characteristic of high $T_C$ DC SQUID

Ya.S. Greenberg[1,a], I.L. Novikov[1], V. Schultze[2], and H.-G. Meyer[2]

[1] Novosibirsk State Technical University, 20 K. Marx Ave. Novosibirsk, 630092, Russia
[2] Institute for Physical High Technology, 07702, Jena, Germany

Received 13 July 2004 / Received in final form 9 December 2004
Published online 16 April 2005 – 

**Abstract.** A theory for the voltage-current characteristic in high $T_C$ DC SQUIDs (Superconducting Quantum Interference Devices), which accounts for a second harmonic in the junction current-phase relation, is developed. It is shown that the small inductance DC SQUIDs can be used for the investigation of the second harmonic via its influence on the voltage-flux curve. If the second harmonic is perceptible, then for large inductance DC SQUIDs the theory can explain the substantial deviations of the experimental voltage modulation from theoretical predictions and computer simulations based on conventional sinusoidal current-phase relation. The detail comparison with the experiment is performed.

**PACS.** 74.50.+r Tunneling phenomena; point contacts, weak links, Josephson effects – 85.25.-j Superconducting devices – 85.25.Dq Superconducting quantum interference devices (SQUIDs)

## 1 Introduction

As is well known, there exists a significant discrepancy between experimental results and numerical simulations of the voltage-to-flux transfer function of high $T_C$ DC SQUIDs [1,2]. This is one of the most important unsolved problems, which seriously hinders the optimization of high $T_C$ DC SQUIDs for applications.

In spite of extensive computer simulations [1,3] and theoretical studies [4–6] that have been performed in the attempt to predict reliably transfer function and energy resolution of high $T_C$ DC SQUIDs, a marked disagreement with experiment still exists: experimental transfer functions in many cases are much lower than the values predicted by theory and computer simulations; the white noise is about ten times higher than predicted.

One of the possible reasons for these discrepancies could be attributed to the junction asymmetry of SQUID interferometer (unequal critical currents or (and) normal resistances), which for grain boundary junctions is about 20%–30% due to on chip technological heterogeneity. However, the junction asymmetry can explain only small deviations from theoretical curves [3,7]. As was shown in [6], the junction asymmetry always results in the increase of the voltage modulation if the junction critical current is greater than approximately 5 $\mu$A. Therefore, the majority of experimental points, cannot be explained by the junction asymmetry.

[a] e-mail: greenbergy@online.nsk.su

Therefore, the problem of large reduction of transfer function and the voltage modulation relative to theoretical predictions is still open.

The other possible reason for aforementioned deviations, which is investigated in the paper, is the influence of a second harmonic in the current-phase relation (CPR) of a high temperature superconducting Josephson junction on the voltage modulation in high $T_C$ DC SQUID.

It is well established now that the CPR in high $T_C$ junctions is non-sinusoidal, possessing a second harmonic component whose relative magnitude depends on mutual orientation of the d-wave superconductors, and whose sign can be temperature dependent [8–10]:

$$I_S = I_1 \sin\varphi + I_2 \sin 2\varphi, \tag{1}$$

where $I_S$ is a supercurrent flowing through the junction, $\varphi$ is a phase difference of the superconducting order parameter across the junction. The amplitude of the first harmonic $I_1$ depends on the relative orientation of d-wave superconductors. In asymmetric 45° [001]-tilt grain boundary junction the amplitude $I_1$ is expected to disappear due to symmetry [11]. In this case the amplitude $I_2$ becomes prominent, and has been observed in direct CPR measurements [12,13], and as a half-flux quantum periodicity of critical current in YBCO DC SQUIDs [14].

More recent studies revealed a substantial amount of a second harmonic also in [001]-tilt grain boundary junction with a 30° asymmetric misorientation angle [15].

In the present paper we investigate the effect of a second harmonic on the voltage-current characteristics (VCC) and on the voltage-flux curves (VFC) of high $T_C$ DC SQUID.

We consider a symmetrical DC SQUID interferometer with nominally equal shunt resistances, $R_1 = R_2 = R$, and with equal amplitudes of each harmonics:

$$I_1^{(1)} = I_1^{(2)} \equiv I_1; \quad I_2^{(1)} = I_2^{(2)} \equiv I_2, \tag{2}$$

where the superscripts refer to the junction number.

The paper is organized as follows. In the Section 2 we consider the DC SQUID with a low geometrical inductance of the interferometer loop. In the approximation of Ambegaokar and Halperin we obtain analytical expressions for the voltage-flux curves. It is shown that the second harmonic results in characteristic distortion of the VFC. In particular, if the first harmonic is absent, the VFC has the half-flux quantum periodicity.

The Section 3 is devoted to DC SQUID with large inductance of the interferometer loop. In the frame of the approach that has been developed earlier [5] we obtain the analytical expression for the VCC which accounts for the influence of the second harmonic. The principal result of the theory is that the admixture of the second harmonic results in the increase of the critical current of DC SQUID and simultaneously in the reduction of the voltage modulation.

The detail comparison of the theory with experiment is given in the Section 4. It is shown that a significant reduction of the modulation signal observed experimentally can be explained by the perceptible admixture of the second harmonic in CPR.

## 2 DC SQUID with small inductance

First detail experimental investigation of the influence of second harmonic on the dynamic behavior of small inductance YBCO DC SQUID with asymmetric 45° grain boundary junctions was performed in [16]. It was shown that the peculiarities in the dependence of critical current on the external flux can be explained by the large amount of second harmonic in the junction CPR.

In this section we obtain the analytical expression for the output voltage of small inductance DC SQUID, which allows one to investigate the SQUID properties in a broad range of temperatures, and of the amplitudes $I_1$ and $I_2$.

Neglecting the inductance of the loop we can write the energy of DC SQUID loop in the external magnetic field:

$$U = -E_J \left( i\varphi + 2\cos\varphi_X \cos\varphi + \gamma \cos 2\varphi_X \cos 2\varphi \right), \tag{3}$$

where $E_J = \Phi_0 I_1/2\pi$ is the Josephson coupling energy, $i = I/I_1$, $I$ is the bias current, $\varphi_X = \pi\Phi_X/\Phi_0$, $\Phi_X$ is the external magnetic flux, $\Phi_0 = h/2e$ is a flux quantum, $\gamma = I_2/I_1$.

As is known, DC SQUID with a negligible small inductance can be considered as a single Josephson junction with normal resistance $R/2$ and doubled critical current. Therefore, we may use the known approach of Ambegaokar and Halperin [17] to account for a second harmonic in the voltage current characteristic of such SQUID at finite temperature:

$$\frac{V}{RI_1} = \frac{\pi\Gamma}{p\left(i, \Gamma, \varphi_X\right)} \tag{4}$$

where $\Gamma = 2\pi k_B T/\Phi_0 I_1$ is the noise parameter, $T$ is the absolute temperature,

$$p\left(i, \Gamma, \varphi_X\right) = \left[ \int_0^{2\pi} e^{-W(y)} dy \int_0^{y} e^{W(x)} dx - \frac{1}{1 - e^{\frac{2\pi i}{\Gamma}}} \int_0^{2\pi} e^{W(x)} dx \int_0^{2\pi} e^{-W(x)} dx \right] \tag{5}$$

$$W(x) = \left(i/\Gamma\right) x + \left(2/\Gamma\right) \cos\varphi_X \cos x + \left(\gamma/\Gamma\right) \cos 2\varphi_X \cos 2x. \tag{6}$$

The expression (4) is valid for any temperature below $T_C$, the critical temperature of a superconductor, however, all calculations we show below have been performed for $T = 77$ K.

The equation (4) is a good approximation for DC SQUIDs with $\alpha \ll 1$, $\beta \ll 1$, where $\alpha = L/L_F$, $L_F = (\Phi_0/2\pi)^2/k_B T$ is a fluctuation inductance which is equal to 100 pH at $T = 77$ K, $\beta = 2LI_1/\Phi_0$. Therefore, in general, SQUID behavior is described by three parameters, $\alpha$, $\beta$, $\Gamma$, but only two are independent due to relation $\alpha = \pi\beta\Gamma$.

The voltage-flux curves (VFC) calculated from the expression (4) are shown in Figure 1. As is seen, the presence of a second harmonic gives rise to the half-flux quantum periodicity of VFC. It also implies the voltage invariance under reversal of the sign of $I_2$. In addition, the second harmonic reduces the modulation depth. Therefore, the purposely made DC SQUID with small inductance ($\alpha \ll 1$, $\beta \ll 1$) can be a convenient device for the investigation of the second harmonic in high $T_C$ superconductors via its influence on the voltage-flux characteristic.

## 3 DC SQUID with large inductance

As is well known the high $T_C$ DC SQUIDs, which are used in practical SQUID systems, have large geometrical inductance of interferometer loop, typically $L > 100$ pH.

Therefore, in this section we consider a DC SQUID with large inductance, $\alpha \geq 1$ and any $\beta$ and $\Gamma$ consistent with the relation $\alpha = \pi\beta\Gamma$. The theory of the voltage-current characteristics for such SQUID has been developed earlier [5]. Here we apply this theory to a SQUID with the second harmonic in junctions CPR. According to the approach of [5] we have obtained the following result for the voltage across a SQUID with a second harmonic in CPR:

$$\frac{V}{RI_1} = J - \exp\left(-\alpha/2\right) \cos(2\varphi_X) f(i, \Gamma, \gamma) \tag{7}$$

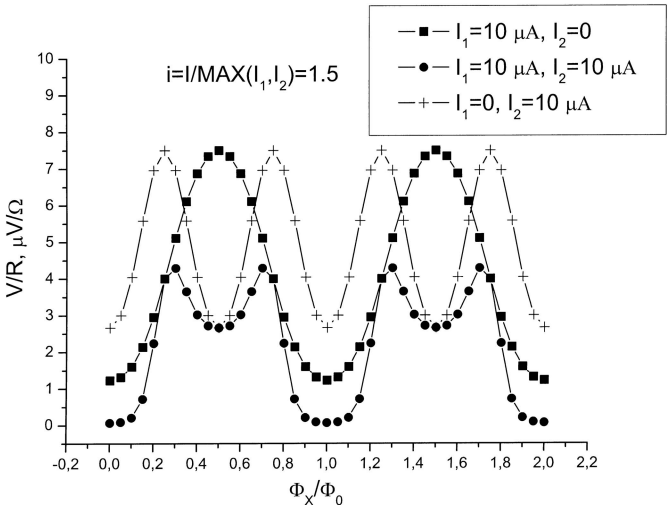


**Fig. 1.** Voltage-flux curves for small inductance DC SQUID calculated from equation (4). (solid square)- $I_1 = 10\ \mu$A, $I_2 = 0$ (2nd harmonic is absent), $i = I/I_1 = 1.5$; (solid circle)- $I_1 = 10\ \mu$A, $I_2 = 10\ \mu$A, $i = I/I_1 = 1.5$; (cross)- $I_1 = 0$, $I_2 = 10\ \mu$A (1st harmonic is absent), $i = I/I_2 = 1.5$.

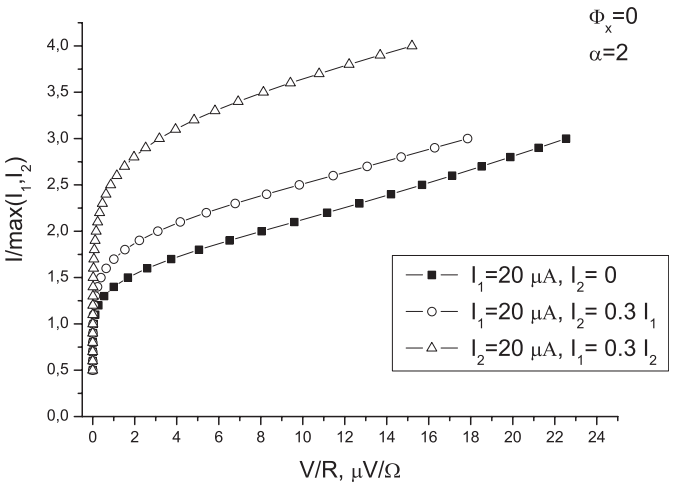


**Fig. 2.** Voltage-current curves for large inductance DC SQUID calculated from equation (7). $L = 2L_{\rm F}$, $\Phi_X = 0$, $\gamma = I_2/I_1$; (solid square)- $I_1 = 20\ \mu$A, $I_2 = 0$; (open circle)- $I_1 = 20\ \mu$A, $I_2 = 0.3\ I_1$; (open triangle)- $I_2 = 20\ \mu$A, $I_1 = 0.3\ I_2$.

where

$$J^{-1} = 2i \sum_{n=-\infty}^{n=+\infty} \frac{(-1)^n\, G_n^+ G_n^-}{i^2 + 4n^2\Gamma^2} \tag{8}$$

$$f(i,\Gamma,\gamma) = 8J^3 \left[ i^2 A\,(A+C) - 4\Gamma^2 B\,(D-B) \right] \tag{9}$$

$$A = \sum_{n=-\infty}^{n=+\infty} \frac{(-1)^n\, G_{n+1}^+ G_n^-}{i^2 + 4n^2\Gamma^2} \tag{10a}$$

$$C = \sum_{n=-\infty}^{n=+\infty} \frac{(-1)^n\, G_n^+ G_{n+1}^-}{i^2 + 4n^2\Gamma^2} \tag{10b}$$

$$B = \sum_{n=-\infty}^{n=+\infty} \frac{(-1)^n\, n G_{n+1}^+ G_n^-}{i^2 + 4n^2\Gamma^2} \tag{10c}$$

$$D = \sum_{n=-\infty}^{n=+\infty} \frac{(-1)^n\, n G_n^+ G_{n+1}^-}{i^2 + 4n^2\Gamma^2} \tag{10d}$$

$$G_n^{\pm} = \sum_{m=-\infty}^{m=+\infty} (\pm 1)^m\, I_{n-2m}\,(1/\Gamma)\, I_m\,(\gamma/\Gamma), \tag{11}$$

where $I_n$ is a modified Bessel function.

The voltage modulation $\Delta V = V(\varphi_X = \pi/2) - V(\varphi_X = 0)$ is readily obtained from (7):

$$\frac{\Delta V}{RI_1} = 2\exp\left(-\alpha/2\right) f(i,\Gamma,\gamma). \tag{12}$$

The expression (7) is valid for $\alpha \geq 1$ and any values of $\beta$ and $\Gamma$, which are consistent with the condition $\alpha = \pi\beta\Gamma$. Therefore, it can be applied for the analysis of a majority of practical high $T_C$ DC SQUIDs with $\Gamma \approx 0.05-1$, $\beta \geq 1$, $\alpha \geq 1$. However, it should be remembered that (7) is the approximate expression which accounts for the first order term in the perturbation expansion of the voltage over small parameter $\varepsilon = \exp(-\alpha/2)$ (see [5]).

Contrary to the case of zero inductance (expression (4)), here VCC (7) is not invariant under sign reversal of $I_2$ since magnetic energy term in the Hamiltonian of DC SQUID, $(\Phi - \Phi_X)^2/2L$, destroys the invariance. Indeed, as follows from (11), $G_n^{\pm}(-\gamma) = G_n^{\mp}(\gamma)$, then, the quantities in (7) transforms as follows: $J \to J, A \to C, C \to A, B \to D, D \to B$. Therefore, $f(i,\Gamma,-\gamma) \neq f(i,\Gamma,\gamma)$. However, for large inductance ($\alpha \geq 1$) the VCC is approximately invariant under sign reversal of $I_2$ since the second term in right hand side of (7) is much smaller than the first one.

If the second harmonic is absent ($\gamma = 0$), then, we have $G_n^{\pm} = I_n(1/\Gamma)$, $C = A$, $D = B$, and we get the result obtained in [5] for symmetric DC SQUID with conventional CPR.

It is interesting to note that if the first harmonic is absent ($I_1 = 0$), then the voltage modulation is, within our approximation, exactly equal to zero. It follows from (11) that for $I_1 = 0$

$$G_n^{\pm} = \begin{cases} (\pm 1)^{n/2}\, I_{n/2}\,(\gamma/\Gamma) & \text{for } n \text{ even} \\ 0 & \text{for } n \text{ odd.} \end{cases} \tag{13}$$

Then, from (10) we have $A = C = D = B = 0$. Therefore, the modulation signal (the second term in (7)) is absent in this case. Of course, it is not a strong statement, since the expression (7) accounts only for the first order term in the perturbation expansion of the voltage over small parameter $\varepsilon = \exp(-\alpha/2)$. However, from these considerations we can expect a significant reduction of the voltage modulation if the second harmonic is perceptible.

The influence of the second harmonic on the voltage-current curve (VCC) is shown in Figure 2. We see that the second harmonic enhances the SQUID critical current. The more the amplitude of the second harmonic the more is the enhancement of the critical current. As is seen

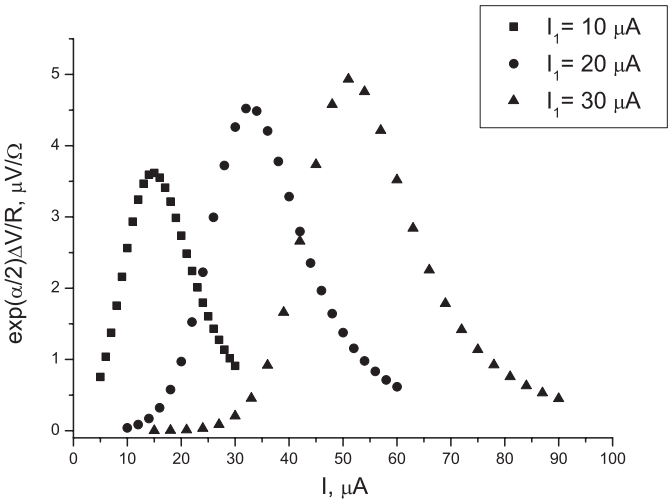


**Fig. 3.** The reduced voltage modulation vs. bias current curves in the absence of the second harmonic (calculated from Eq. (12)). (solid square)- $I_1 = 10\ \mu$A; (solid circle)- $I_1 = 20\ \mu$A; (solid triangle)- $I_1 = 30\ \mu$A.

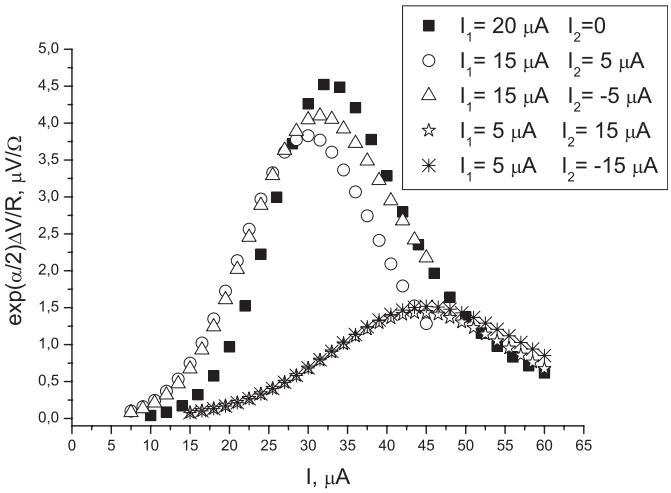


**Fig. 4.** The influence of the second harmonic on the voltage modulation. (solide square)- $I_1 = 20\ \mu$A, $I_2 = 0$; (open circle)- $I_1 = 15\ \mu$A, $I_2 = 5\ \mu$A; (open triangle)- $I_1 = 15\ \mu$A, $I_2 = -5\ \mu$A; (open stars) $I_1 = 5\ \mu$A, $I_2 = 15\ \mu$A; (*)- $I_1 = 5\ \mu$A, $I_2 = -15\ \mu$A.

from Figure 2, for given value of the sum, $I_1 + I_2$, the critical current is greatly enhanced, if the second harmonic is perceptible.

As is seen from (12) the influence of inductance on the voltage modulation is factored out, so that below we consider the reduced modulation $\exp(\alpha/2)\Delta V/R$, which depends on the bias current I and harmonic amplitudes $I_1$ and $I_2$.

In the absence of the second harmonic ($I_2 = 0$) the reduced voltage modulation vs. current curves, $\Delta V(I)$ have the form as shown in Figure 3. For a given junction critical current $I_1$ the curve has a well defined maximum $\Delta V(I_{\rm MAX}) = \Delta V_{\rm MAX}$ at the corresponding value of the bias current $I = I_{\rm MAX}$.

Our calculations show that the admixture of a second harmonic independently of its sign reduces the voltage modulation as is seen from Figure 4. A significant reduction is obtained only if the amplitude of the second harmonic is several times that of the first harmonic. However, the forms of the curves are similar to those for $\gamma = 0$: on the bias current axes they have one maximum, which position is shifted to lower bias currents for relatively small admixture of the second harmonic, and to the higher bias currents if the amount of the second harmonic is significant.

For the practical purpose it is convenient to have a set of the values of maximum voltage modulation $\Delta V_{\rm MAX}$ with a corresponding values of the bias current $I_{\rm MAX}$. Just these two quantities can easily be measured in practice: by varying the bias current the point of maximum voltage modulation $\Delta V_{\rm MAX}$ is being obtained at particular value of bias current $I = I_{\rm MAX}$.

From equation (12) for a set of two fixed values, $I_1$ and $\gamma$ we computed a set of the values of maximum voltage modulation $\Delta V_{\rm MAX}$ with a corresponding values of bias current $I_{\rm MAX}$. The dependences $\Delta V_{\rm MAX}(I_{\rm MAX})$ are shown for several $\gamma'$-s in Figure 5. The different points on

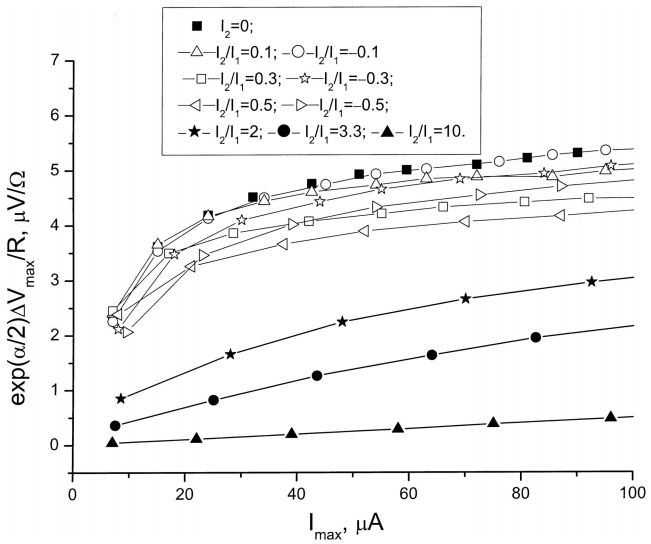


**Fig. 5.** The dependence of maximum voltage modulation on the bias current. The influence of second harmonic. (solid square)- $I_2 = 0$; (open triangle)- $I_2/I_1 = 0.1$; (open circle)- $I_2/I_1 = -0.1$; (open square) $I_2/I_1 = 0.3$; (open stars)- $I_2/I_1 = -0.3$; (left corner open triangle)- $I_2/I_1 = 0.5$; (right corner open triangle)- $I_2/I_1 = -0.5$; (solid stars)- $I_2/I_1 = 2$; (solid circle)- $I_2/I_1 = 3.3$; (solid triangle)- $I_2/I_1 = 10$.

a particular curve belong to different values of $I_1$ in the range $5\ \mu\text{A} \leq I_1 \leq 50\ \mu$A. As it follows from Figure 5, a relative small portion of the second harmonic gives rise to a relative small reduction of the voltage modulation as compared to that for the conventional CPR. A substantial reduction is obtained only if the second harmonic is strongly pronounced. The reduction of the voltage modulation is not invariant under the change of the sign of $\gamma$. As is seen from Figure 5, the reduction for positive $\gamma'$-s is more pronounced.

## 4 Comparison with experiment

In order to compare our theory with experiment we took a couple of DC SQUIDs with $\alpha \geq 1$ and $\Gamma \geq 0.05$ out of those which have been chosen before for the same purpose [7]. All of these SQUIDs are single layer ones, using 100 or 200 nm thick $YBa_2Cu_3O_{7-x}$ films deposited by laser ablation onto $SrTiO_3$ bicrystal substrates with 24° or 30° misorientation angles, both having symmetrical configuration. The technology is described in detail in [18]. The SQUID layouts cover small SQUIDs either used solo [19] or directly coupled to a pickup loop [20]. In any case, the investigated SQUIDs are formed by slim loops as shown in Figure 6.

All measurements were performed in liquid nitrogen at 77 K.

The experimental results shown in Figures 7a, b are drawn with error bars, representing the uncertainties of the measurements. Maximum voltage modulation $\Delta V_{\mathrm{MAX}}$ and corresponding bias current, $I_{\mathrm{MAX}}$, are measured directly. Therefore, their errors amount to maximum 0.5 $\mu$V and 0.5 $\mu$A, respectively. The normal resistance $R$ was determined by fitting the VCC at high currents. The error is as low as 0.1 Ω. In the parameter $\alpha = L/L_F$ the fluctuation inductance $L_F$ is exact, but the SQUID inductance $L$ may contain errors.

Only the kind of SQUID shown in Figure 6 is included in the results shown in Figures 7a, b. This SQUID type is at the very end intended to be used for direct coupling of a pickup loop. Here the fraction $kL$, where some injection current $I_i$ flows around the SQUID loop, can be determined directly by measurement with the expression $kL = \Phi_0/I_i$. Here $I_i$ is that injection current which is needed to produce one modulation period, thus representing one $\Phi_0$, in the voltage-flux curve. Then, $kL$ was calculated by a numerical method described in [21]. For theses calculations, the geometry is given and the actual YBCO thickness is used. Because the calculation also includes the kinetic inductance, the free fitting parameter is the London penetration depth. Its value has to be constant for any SQUID on the same substrate. There were always five or more SQUIDs on each substrate, mostly having different layout (slit length, rim width). The deviation between measured and calculated $kL$ was always below 10% for all the different layouts. Therefore, also the complete SQUID inductance $L$, calculated with the same parameters, will be within this error margin.

As is seen from Figure 7a, most of experimental points lie well below the curve for DC SQUID with conventional CPR. Out of them, only few would need a very strong contribution of the second harmonics in order to explain their extremely low voltage modulation (see Fig. 7b). Most of the experimental data could be explained by a moderate contribution of the second harmonics in the CPR. There is no remarkable difference between the SQUIDs using 24° or 30° bicrystals.

Yet, there exist few experimental points which lie above the conventional CPR curve. Our theory cannot explain these points, since the admixture of the second harmonic always leads to the reduction of the voltage modulation. Looking for any other possible parameter which could enhance the voltage modulation, asymmetry between the two Josephson junctions of the SQUID could be taken into account. In [6] it was shown that for relatively large critical current of the junction ($\geq$5 $\mu$A) the junction asymmetry always leads to an enhancement of the voltage modulation. With a typical critical current spread of about 30% of our junctions on one bicrystal substrate [22] such extraordinarily high modulation values should be explainable.

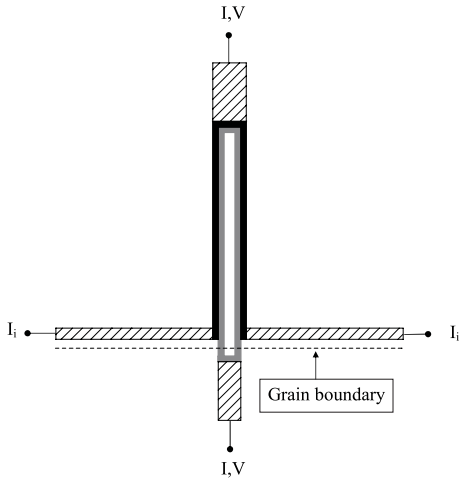


**Fig. 6.** Layout of the investigated SQUIDs. The SQUIDs are formed by a slim loop, using grain boundary junctions. Slit length and rim width are varied. I,V denote the terminals for the SQUID characterization. An injection current $I_i$ is fed into the loop. The black crook denotes the coupling inductance $kL$; the grey loop-the whole SQUID inductance $L$.

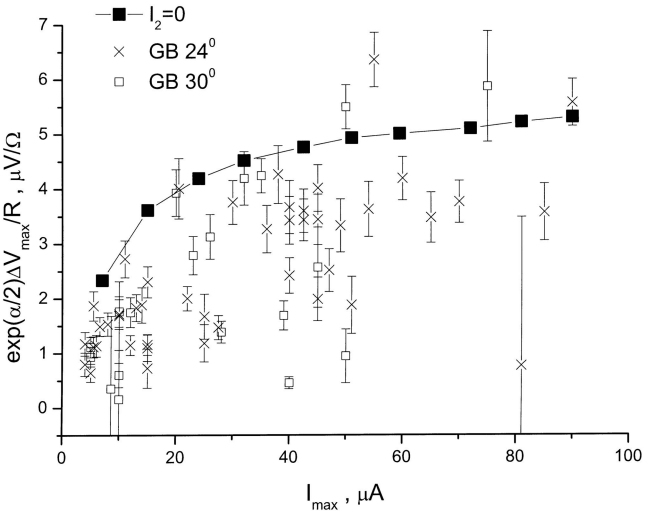


**Fig. 7a.** Experimental voltage modulation for YBCO grain boundary junctions with symmetric misorientation angles (cross- 24°, open square- 30°). The conventional CPR curve ($I_2 = 0$), which is shown by solid squares, denotes the upper bound for the voltage modulation of symmetric DC SQUID.

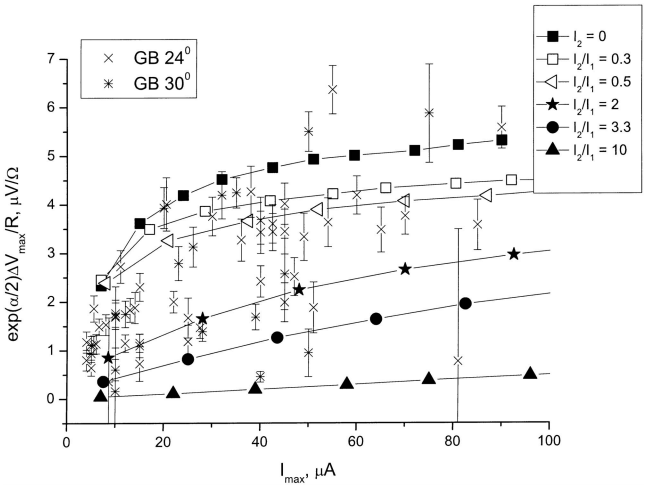


**Fig. 7b.** Experimental voltage modulation for YBCO grain boundary junctions with symmetric misorientation angles (cross- 24°, snowflake- 30°). The conventional CPR curve ($I_2 = 0$), which is shown by solid squares, denotes the upper bound for the voltage modulation of symmetric DC SQUID. (open square)- $I_2/I_1 = 0.3$; (left corner open triangle)- $I_2/I_1 = 0.5$; (solid star)- $I_2/I_1 = 2$; (solid circle)- $I_2/I_1 = 3.3$; (solid triangle)- $I_2/I_1 = 10$.

For two of the SQUIDs with such high modulation values shown in Figure 7a, some more data were still available (the two 24° SQUIDs at $I_{\max} = 55$ and 90 $\mu$A, respectively). With the flux shift $\Delta\Phi$ between the VFC at positive and negative bias, using the well-known relation $\Delta\Phi = L(I_{c1} - I_{c2})$, a current asymmetry of $\xi = (I_{c1} - I_{c2})/(I_{c1} + I_{c2}) = 0.16$ is determined for both SQUIDs. Together with their noise parameter of $\Gamma = 0.06$, corresponding to the results in [6], a voltage modulation enhancement of about 10% is originated, which could explain the position of these two points in Figures 7a, b.

## 5 Conclusion

We have shown in the paper that the significant reduction of the voltage modulation in high $T_C$ DC SQUIDs, which lie well below the theoretical predictions and computer simulations based on conventional sinusoidal CPR, can be explained by the presence of relatively large amplitude of a second harmonic in the junction CPR.

Although, the existence of second harmonic in high $T_C$ grain boundary junctions follows from the theory [8–10], and there exist some mechanisms (phase fluctuations between d- and s-wave pairing; faceted structure of grain boundary) that can enhance the contribution of second harmonic [23,24], up to now a reliable evidence of substantial second harmonic was observed only in [001]-tilt grain boundary junction with 45° and 30° asymmetric misorientation angle [12–16]. Therefore, we cannot rule out other mechanisms, which lead to the reduction of the voltage modulation in high $T_C$ DC SQUIDs.

For an unambiguous clarification of the parameters influencing the voltage modulation, a directed manufacturing and analysis of high $T_C$ DC SQUIDs would be deserving.

The authors are grateful to Evgeni Il'ichev and Miroslav Grajcar for fruitful discussions. The work is partly supported by INTAS Program of EU under grant 2001-0809.

## References

1. D. Koelle, R. Kleiner, F. Ludwig, E. Dantsker, J. Clarke, Rev. Mod. Phys. **71**, 631 (1999)
2. A.I. Braginski, K. Barthel, B. Chesca, Ya.S. Greenberg, R. Kleiner, D. Koelle, Y. Zhang, X. Zeng, Physica C **341-348**, 2555 (2000)
3. J. Muller, S. Weiss, R. Gross, R. Kleiner, D. Koelle, IEEE Trans. Appl. Supercond. **11**, Pt. 1, 912 (2001)
4. B. Chesca, J. Low Temp. Phys. **112**, 165 (1998)
5. Ya.S. Greenberg, Physica C **371**, 156 (2002)
6. Ya.S. Greenberg, Physica C **383**, 354 (2003)
7. Ya.S. Greenberg, H.-G. Meyer, V. Schultze, Physica C **368**, 236 (2002)
8. Yu.S. Barash, A.V. Galaktionov, A.D. Zaikin, Phys. Rev. Ser. B **52**, 665 (1995)
9. W. Zhang, Phys. Rev. B **52**, 3772 (1995)
10. Y. Tanaka, S. Kashiwaya, Phys. Rev. B **53**, R11957 (1996)
11. M. Sigrist, T.M. Rice, J. Phys. Soc. Jpn **61**, 4283 (1992)
12. E. Il'ichev, V. Zakosarenko, R. Ijsselsteijn, V. Schultze, H.-G. Meyer, H.E. Hoenig, Phys. Rev. Lett. **81**, 894 (1998)
13. E. Il'ichev, V. Zakosarenko, R. Ijsselsteijn, H.E. Hoenig, V. Schultze, H.-G. Meyer, M. Grajcar, R. Hlubina, Phys. Rev. B **60**, 3096 (1999)
14. C.W. Schneider, G. Hammer, G. Logvenov, T. Kopp, J.R. Kirtley, P.J. Hirschfeld, J. Mannhart, Europhys. Lett. **68**, 86 (2004)
15. C.H. Gardiner, R.A.M. Lee, J.C. Gallop, A.Ya. Tzalenchuk, J.C. Macfarlane, L. Hao, Supercond. Sci. Technol. **17**, S234 (2004)
16. T. Lindstrom, S.A. Charlebois, A.Ya. Tzalenchuk, Z. Ivanov, M.H.S. Amin, A.M. Zagoskin, Phys. Rev. Lett. **90**, 117002 (2003)
17. V. Ambegaokar, B.I. Halperin, Phys. Rev. Lett. **22**, 1364 (1969)
18. R. Ijsselsteijn, H. Elsner, W. Morgenroth, V. Schultze, H.-G. Meyer, IEEE Trans. on Appl. Supercond. **9**, 3933 (1999)
19. J. Ramos, V. Zakosarenko, R. Ijsselsteijn, R. Stolz, V. Schultze, A. Chwala, H.E. Hoenig, H.-G. Meyer, Supercond. Sc. Technol. **12**, 597 (1999)
20. V. Schultze, V. Zakosarenko, R. Ijsselsteijn, J. Ramos, H.G. Meyer, IEEE Trans. on Appl. Supercond. **9**, 3279 (1999)
21. G. Hildebrandt, F.H. Uhlmann, IEEE Trans. on Magnetics **32**, 690 (1996)
22. V. Schultze, R. Ijsselsteijn, H.-G. Meyer, J. Oppenlander, C. Haussler, N. Schopohl, IEEE Trans. Appl. Supercond. **13**, 775 (2003)
23. R. Hlubina, M. Grajcar, E. Il'ichev, in *Studies of High Temperature Superconductors, Cuprates and Some Unconventional Systems*, edited by A. Narlikar (Nova Science Publishers, New York, 2003)
24. R. Hlubina, M. Grajcar, J. Mraz, e-print archive: `cond-mat/0304213` (2003)